

## **Supporting Information:**

# **Core-Shell Nanoparticle-Based Peptide Therapeutics and Combined Hyperthermia for Enhanced Cancer Cell Apoptosis**

Birju P. Shah<sup>a</sup>, Nicholas Pasquale<sup>a</sup>, Gejing De<sup>b</sup>, Tao Tan<sup>b</sup>, Jianjie Ma<sup>a</sup> and Ki-Bum Lee<sup>a\*</sup>

[<sup>a</sup>] Birju P. Shah, Nicholas Pasquale and Prof. Ki-Bum Lee

Department of Chemistry and Chemical Biology

Rutgers University

Piscataway, NJ 08854 (USA)

Fax: (+1)732-445-5312

E-mail: [kblee@rutgers.edu](mailto:kblee@rutgers.edu)

Homepage: <http://rutchem.rutgers.edu/~kbleeweb/>

[<sup>b</sup>] Gejing De, Tao Tan, and Prof. Jianjie Ma

Department of Surgery

The Ohio State University Medical Center

## SUPPORTING FIGURES

- Figure S1** Biocompatibility of MCNPs in glioblastoma cells
- Figure S2** Biocompatibility of MCNPs in MDA-MB-231 cells
- Figure S3** Biocompatibility of MCNP-PEI constructs in U87-vIII and MDA-MB-231 cells
- Figure S4** Effect on cell viability of ATAP in DMSO
- Figure S5** Optimization of magnetic-field exposure time for MCNP-ATAP constructs
- Figure S6** Percent cell viability of cleavable and non-cleavable MCNP-ATAP constructs
- Figure S7** Percent cell viability of MCNP-ATAP constructs combined with water-bath hyperthermia in brain cancer cells.
- Figure S8** Effect of duration of MCNP-mediated hyperthermia on the viability of U87vIII and MDA-MB-231 cells
- Figure S9** Effect of ATAP in DMSO on mitochondrial membrane permeabilization
- Figure S10** Flow cytometry-based Annexin-V/PI assay for evaluating apoptosis in MCNP-ATAP treated cells
- Figure S11** Preliminary *in vivo* studies of ATAP-iRGD constructs in a mouse model of esophageal cancer.

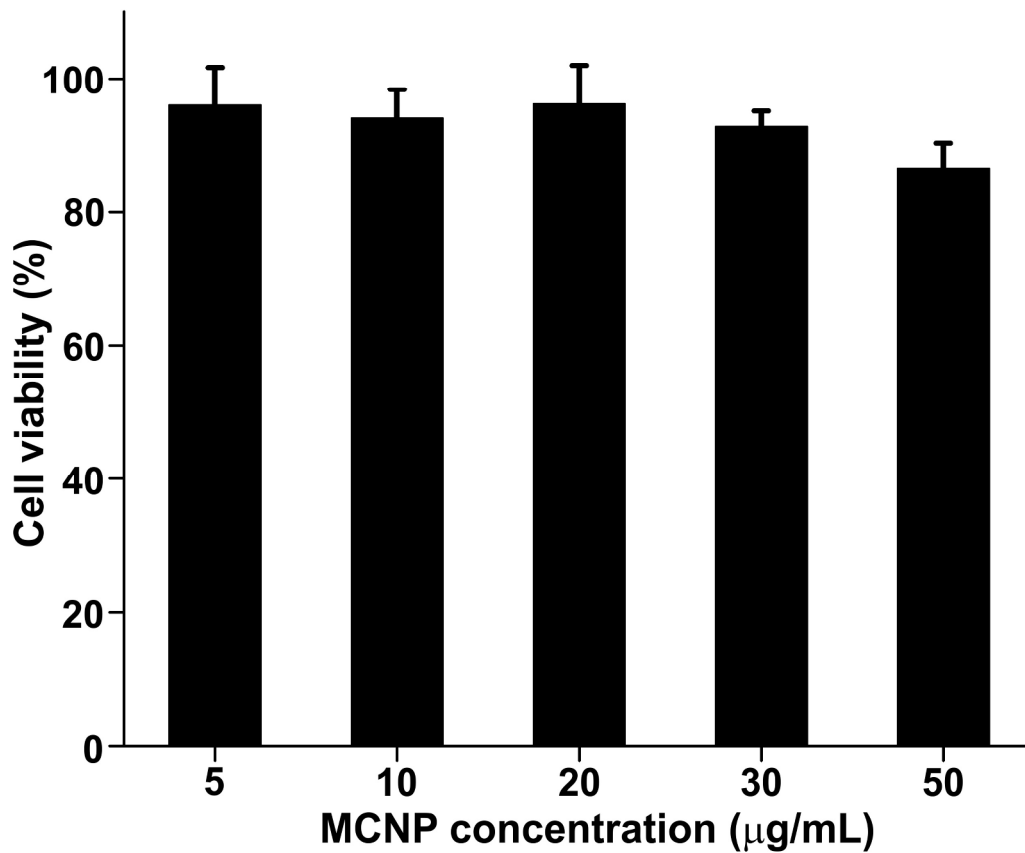


**Figure S1: Biocompatibility of MCNPs in glioblastoma cells.** The percentage of viable cells was estimated using MTS assay following incubation of cells with the MCNPs for 48 h. The data was obtained as absorbance of water-soluble formazan at 490 nm in the MCNP-treated cells, normalized to that of untreated controls. All measurements were done in triplicates and the results represent mean  $\pm$  standard error of mean.

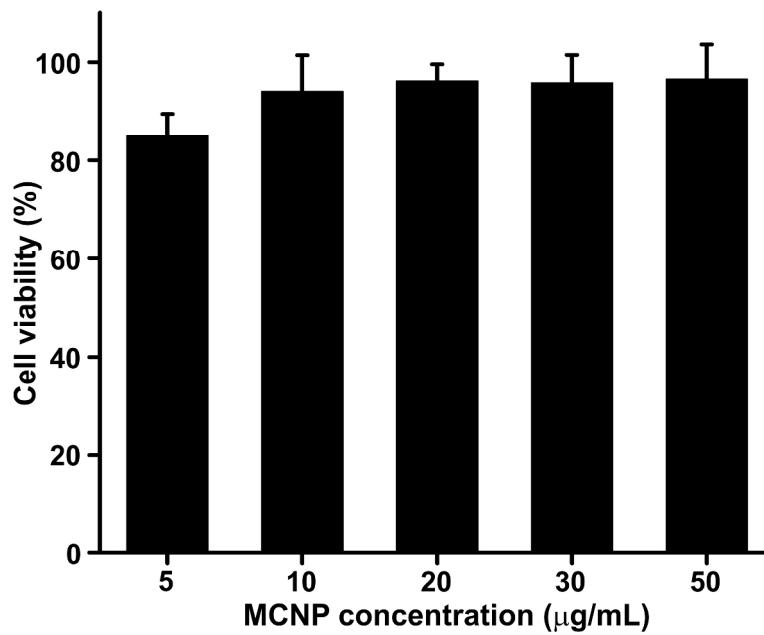


**Figure S2: Biocompatibility of MCNPs in breast cancer cells (MDA-MB-231).** The percentage of viable cells was estimated using MTS assay following incubation of cells with the MCNPs for 48 h. The data was obtained as absorbance of water-soluble formazan at 490 nm in the MCNP-treated cells, normalized to that of untreated controls. All measurements were done in triplicates and the results represent mean  $\pm$  standard error of mean.

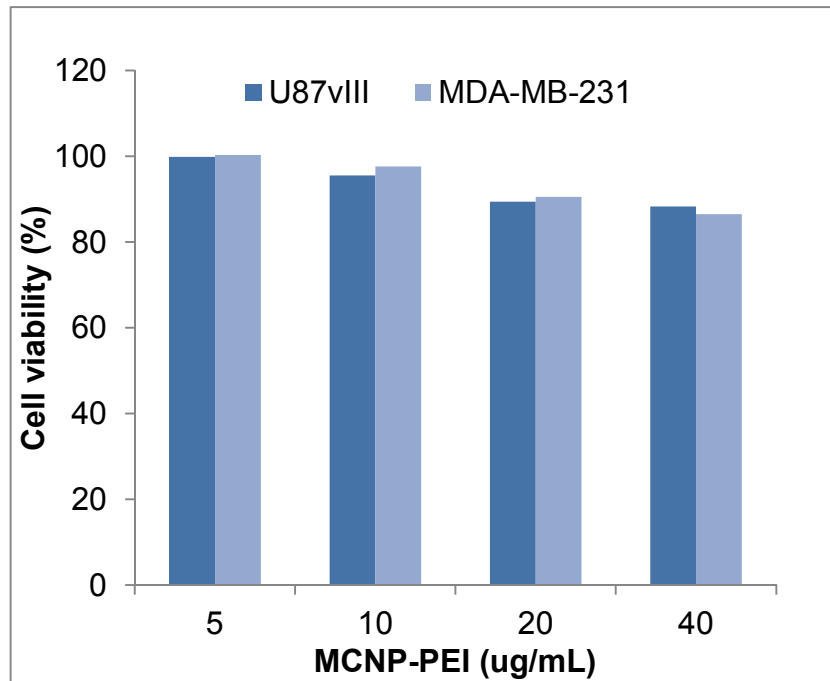


**Figure S3: Biocompatibility of MCNP-PEI constructs in U87vIII and MDA-MB-231 cells.** U87-vIII and MDA-MB-231 cells were treated with varying concentrations of MCNP-PEI constructs. The percentage of viable cells was estimated using MTS assay following incubation of cells with ATAP for 48 h. The data was obtained as absorbance of water-soluble formazan at 490 nm in the MCNP-PEI-treated cells, normalized to that of untreated controls. All measurements were done in triplicates and the results represent mean  $\pm$  standard error of mean.

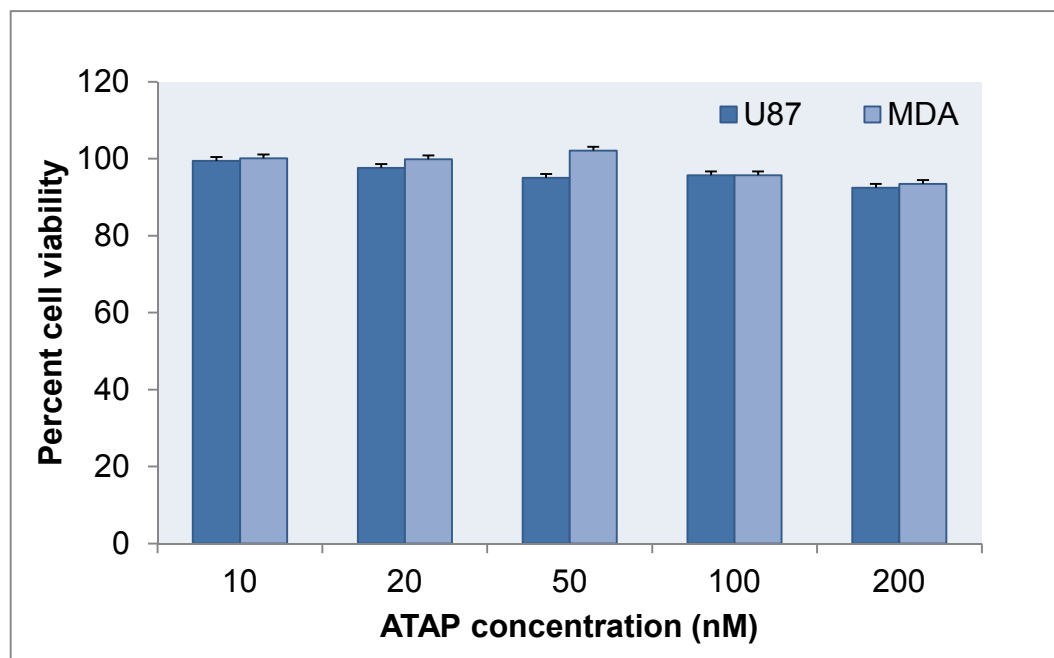


**Figure S4: Effect of cell viability of ATAP dissolved in DMSO.** U87-vIII and MDA-MB-231 cells were treated with varying concentrations of ATAP dissolved in DMSO. The percentage of viable cells was estimated using MTS assay following incubation of cells with ATAP for 48 h. The data was obtained as absorbance of water-soluble formazan at 490 nm in the ATAP-treated cells, normalized to that of untreated controls. All measurements were done in triplicates and the results represent mean  $\pm$  standard error of mean.

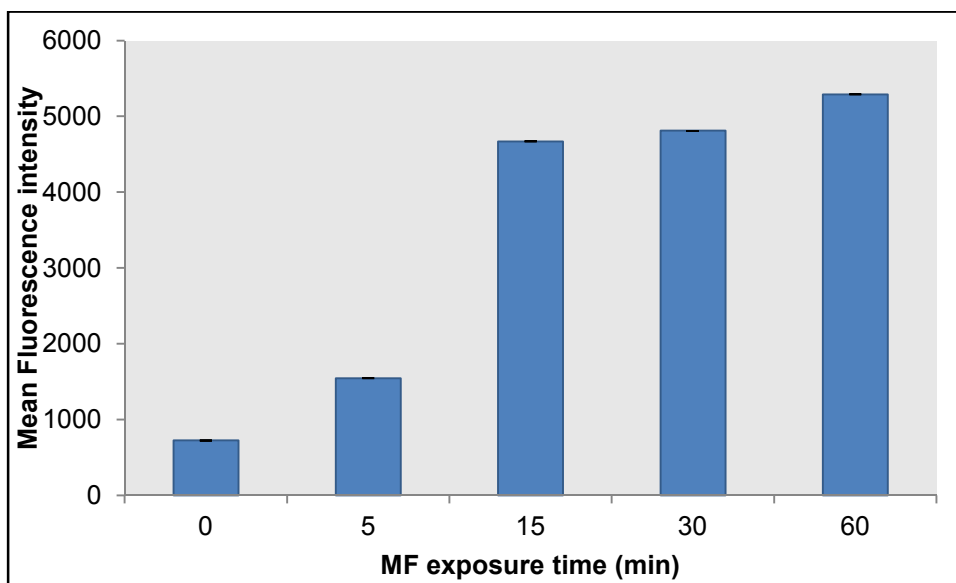


**Figure S5: Effect of magnetic field exposure on the uptake of MCNP constructs.** The MCNPs were coated with PEI first and then labeled with Alexa-Fluor 594. The U87vIII were incubated with 10 ug/mL MCNPs and exposed to a static magnetic field for increasing periods of time (15-60 min). Following this, the cells were washed with cold PBS and replaced with fresh growth medium. The uptake of MCNPs was measured using fluorescence microscopy.

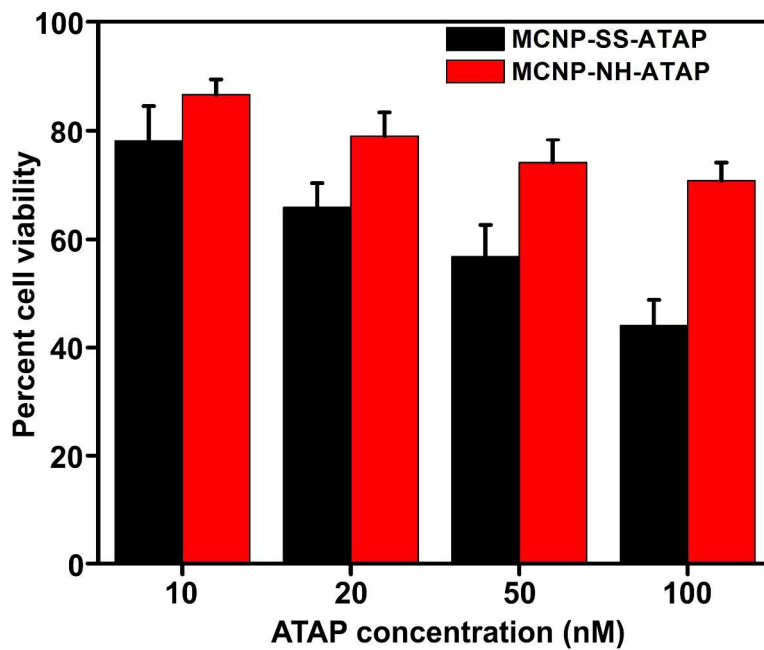


**Figure S6: Percent cell viability of cleavable and non-cleavable MCNP-ATAP constructs.** The brain tumor (U87vIII) cells were treated with MCNP-SS-ATAP (redox-responsive; cleavable) and MCNP-NH-ATAP (non-cleavable) constructs and exposed to a static magnetic field for 30 min. 48 h post transfection, the percent cell viability of the cells was quantified using the MTS cell viability assay. The results represent the average and standard error of mean of three independent experiments

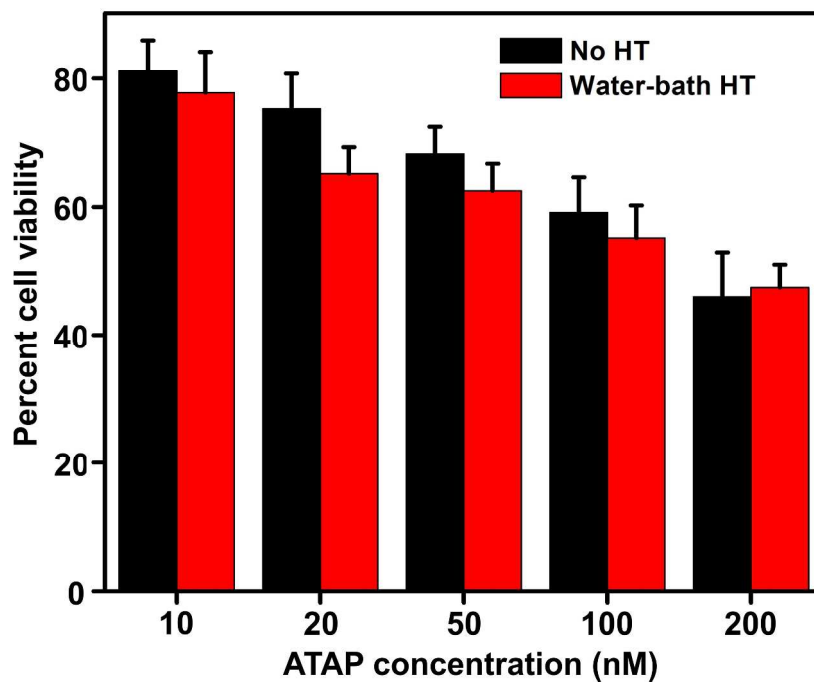


**Figure S7: Percent cell viability of MCNP-ATAP constructs combined with water-bath hyperthermia in brain cancer cells.** The malignant brain cancer (U87vIII) cells were treated with increasing concentrations MCNP-ATAP (No HT) and MCNP-ATAP (with water-bath HT, 45 min) 48 h post transfection, the percent cell viability of the cells was quantified using the MTS cell viability assay. The results represent the average and standard error of mean of three independent experiments. HT, Hyperthermia; MCNP-Magnetic core-shell nanoparticles

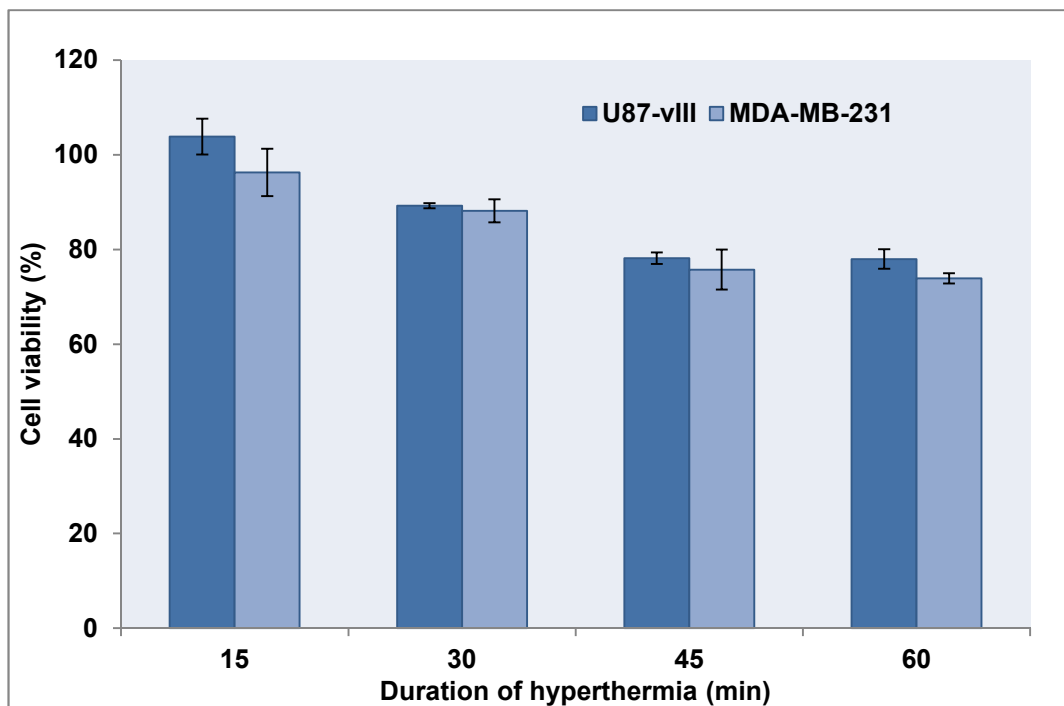


**Figure S8: Effect of duration of MCNP-mediated hyperthermia on the viability of U87-vIII and MDA-MB-231 cells.** The cells were treated with MCNPs (20  $\mu\text{g}/\text{mL}$ ) for 6-8 h, following which the cells were incubated at 37 C for 24 h. After 24 h, the cells were trypsinized and then subjected to different durations of hyperthermia. Cell viability was determined using MTS cell proliferation assay 24 h post hyperthermia treatment (and 48 h post transfection).

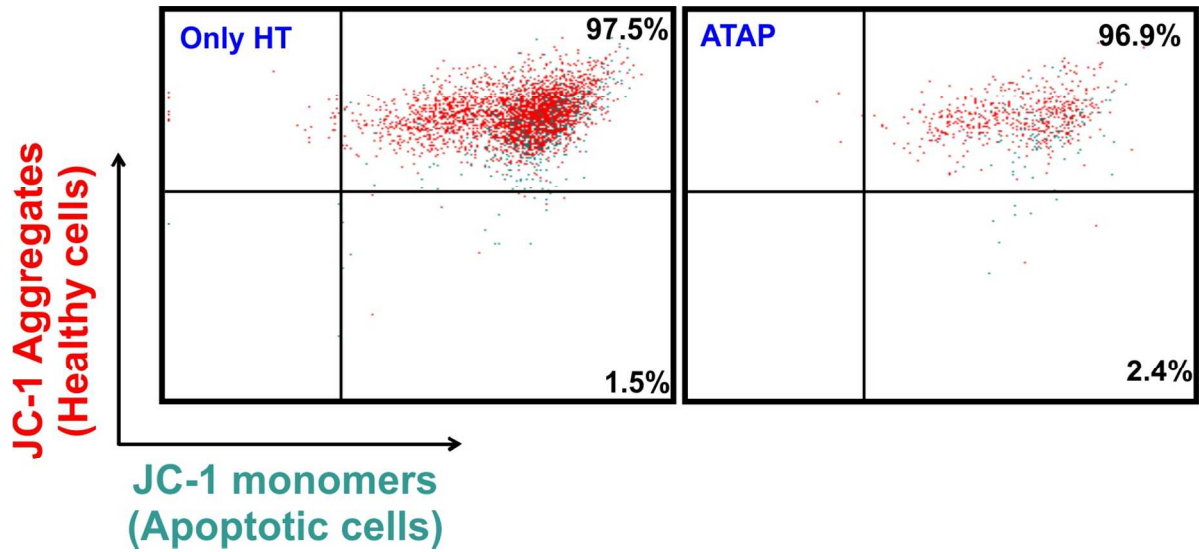


**Figure S9: JC-1 assay for determining mitochondrial membrane permeability of U87-vIII cells.** The cells were incubated with ATAP in DMSO (100 nM) or were exposed to hyperthermia (45 min). 48 h after the treatments, the cells were analyzed according to standard JC-1 protocol using flow cytometry.

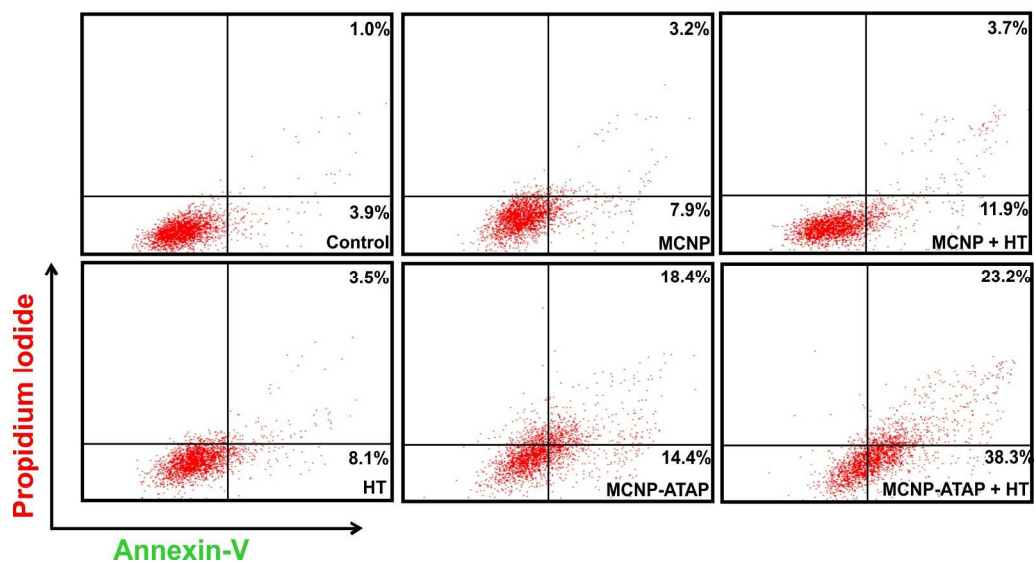


**Figure S10: Flow cytometry-based Annexin-V-FITC/PI assay indicating percentage of early and late apoptotic cells in case of each treatment.** The bottom right quadrant indicates early apoptotic cells (Annexin-V +/PI -); whereas the top right quadrant indicates late apoptotic cells (Annexin-V +/ PI +).

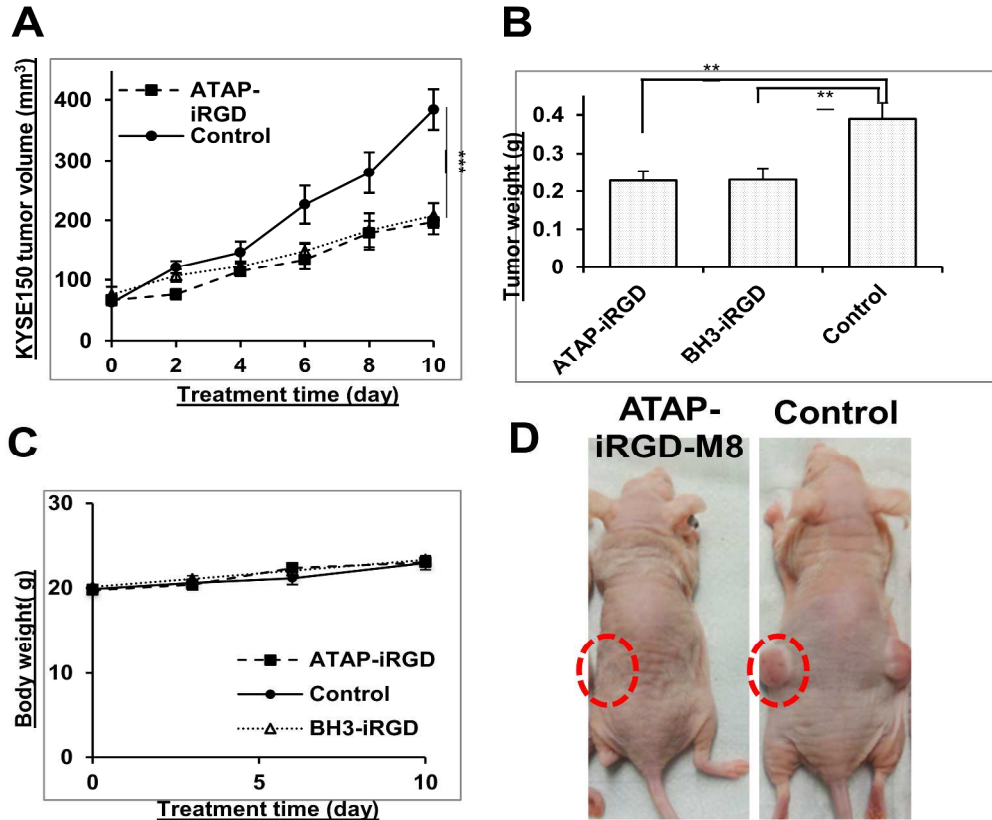


**Figure S11: Preliminary *in vivo* studies of ATAP-iRGD constructs in a mouse model of esophageal cancer.** ATAP-iRGD suppresses esophageal tumor growth with limited off-target toxicity in the mouse model. Esophageal cancer cells KYSE-150 were injected subcutaneously into both flanks of nude mice and allowed to establish tumors. Xenograft model showed that ATAP-iRGD had similar tumor suppression effects as BH3-iRGD peptide (equal molar concentration). Both ATAP-iRGD and BH3-iRGD treatment significantly reduced tumor size and weight (A, B, D), without apparent toxicity and showing no significant difference between the body weights of these three groups (C). Based on MTS assay, the IC<sub>50</sub> for ATAP-iRGD is determined in the range of 1-5 μM in different cancer type (De et al, 2014). After MCNP packaging of ATAP, we found that MCNP-ATAP remarkably improved the IC<sub>50</sub> from the μM range to 50-100 nM range. This shows that utilization of MCNP could enhance the delivery of ATAP to tumor cells.